POAC'23
Glasgow, United Kingdom

Proceedings of the 27th International Conference on
Port and Ocean Engineering under Arctic Conditions
12-16 June 2023, Glasgow, United Kingdom

Modelling ice cover stability in response to wind forcing

McKenna, R.F.[1], Crocker, G.B.[2] and Croasdale, K.R.[3]

[1] R.F. McKenna Associates, Wakefield, QC, CANADA
[2] Dept. of Geography and Environmental Studies, Carleton Univ., Ottawa, ON, CANADA
[3] K.R. Croasdale and Associates, Calgary, AB, CANADA

ABSTRACT

The initiation of movement for a stationary ice cover can be difficult to predict when the ice is anchored at shore, islands, stamukhi and other grounded rubble features within the ice cover. Building on experience in the shallow water ice regime of the north Caspian Sea, an approach has been developed to address this issue. The balance of wind stresses and the above resisting forces has been represented at a resolution of approximately 1 km in a finite element model. The ice is represented as an elastic material with randomly oriented cracks, which effectively prevents the transmission of tensile stresses. Spatially-varying seafloor elevations are represented, as well as spatially and temporally varying water surface elevations. Examples are shown to illustrate basic model behaviour.

KEY WORDS: Ice; Cover; Stability; Wind; Forcing

INTRODUCTION

This paper deals with the initiation of movement for a stationary ice cover that might be restrained by the shore or islands, or through contact with the lake, river or sea floor. While not an easy problem to solve in practice, the concept is straightforward – the cover ice will move when the applied forces exceed the restraining forces.

Circumstances where the initiation of ice movement can be important include mesoscale ice prediction and forecasting models, spring breakup in bays and inlets, and the stability of an ice cover as it affects navigation channels, ice regime and ice forces on structures. Past situations where ice motion has taken place can be observed, whether by means of direct or remote observations of displacements or ice cover characteristics. Remotely sensed imagery, drift beacons and profiling sonar can be very useful in this respect. Occasionally, survey instruments have been used to monitor movements by stakes or beacons placed on the ice surface. Regardless of whether good measurements are available, a representation of the ice cover and the forces acting on it can be useful. A simple approach is to sum the time varying environmental forces (winds, currents) and resistances to identify the circumstances where the total resistance is exceeded. When the stresses transmitted through the ice cover or other parameters influence the forces or resistances, more complex approaches can be necessary.

Over the last 20 years, we have dealt with numerous circumstances where ice cover mobility has been a factor in the north Caspian Sea. This part of the Caspian Sea is less than 5 m deep over tens of kilometres and the ice is anchored to shore (beach sediment, ice or frozen soil,

vegetation), to grounded features (ridges, rubble fields, stamukhi), to natural islands and shoals, and to artificial islands and berms. The ice cover is typically less than 0.5 m thick, with many cracks and small ridges on a scale of a few hundred metres. Most years, winter water levels can rise or fall by 1 m as a result of storm surges and changes of 20 cm or more can take place multiple times over the course of a winter. While ice movement events are often associated with high winds and changes in water level, clear relationships have not been established. When artificial islands and ice protection structures, including berms, are proposed, previous local measurements of ice cover stability are not necessarily representative. In this paper, we have developed a modelling approach to address the initiation of ice movement in the north Caspian Sea and similar ice environments. While Caspian ice conditions have been an impetus for the approach described in the present paper, we have not used any site-specific nor any proprietary data for this effort. An application of this model to Caspian Sea conditions is provided in McKenna et al (2023).

Key aspects of the model include the characterization of resistance to ice motion at islands, stamukhi and partially grounded rubble features, and at shore. The ice cover is represented using continuum finite elements and gap elements are used to prevent the transmission of tensile stresses on a scale of about 1 km. Seafloor elevation, water surface elevation and wind stresses are represented spatially, and both water surface and wind can be varied temporally. Although currents are included in the model, they are negligible for the most part in the Caspian Sea and not described in the paper.

FORCES AGAINST ISLANDS AND GROUNDED ICE FEATURES

Experience in the Caspian Sea and elsewhere suggests that an ice rubbling mechanism is often appropriate for representing the force exerted by relatively thin ice covers over loaded widths of 50 m or more. Various equations based on data from the Canadian Beaufort Sea are given in ISO 19906 (2019), Palmer and Croasdale (2013) and Croasdale (2012). In these relationships, the rubbling load per unit loaded width is a function of the ice thickness, $h^{1.1}$ or $h^{1.25}$, and decreasing with loaded width, $W^{-0.5}$. The rubbling load from Palmer and Croasdale (2013, Equation 5.2.7) for grounded ice rubble is

$$F_B = f\, C_B\, W^{0.5}\, h^{1.1} \tag{1}$$

where C_B is a constant (= 4.8 x 10^6 for F_B expressed in N), h is the local ice thickness and W is the loaded width. Although grounding is frequent in the north Caspian Sea, it need not be a factor in all circumstances and the choice of rubbling model in other circumstances should reflect local conditions. Equation (1) was developed to obtain forces on different structures for use in design. Whereas the strategy for design is the consideration of upper-bound forces, the initiation of failure in the present case more likely involves lower-bound forces. Calculations using ISO 19906 (2019, Equations A.8-41 to A.8-48) suggest that significant rubble accumulation would be required to achieve the load levels predicted by Equation (1). As a result, the reduction factor, f, has been introduced to provide a lower-bound estimate of the rubbling load. In this paper, we have chosen f = 0.5, which should be verified with field data in future.

Expressed simply, the horizontal resistance to sliding of a grounded ice feature on the sea floor is

$$F_G = \mu_{is}\, g\, (1 - p)\, (\rho_i\, H - \rho_w\, d)\, \pi\, D^2/4 \tag{2}$$

where p is the rubble porosity (assumed to be equal above and below water), H is the average thickness of the feature, D is the effective diameter of the feature in plan, d is the water depth, g is the acceleration due to gravity, ρ_i is the ice density and ρ_w is the water density. The factor μ_{is} is the ratio of horizontal resistance to the vertical force applied by the ice feature on the seabed. We have assumed an ice porosity of 0.25, an ice-soil friction coefficient of 0.3, an ice density of 900 kg m^{-3} and a water density of 1006 kg m^{-3} in the calculations presented in this paper. A different approach should be used for cohesive soils.

Equations (1) and (2) are illustrated in Figure 1 for the typical parameters listed above. The rubbling force at an island or stationary ice feature (e.g. stamukha) with a waterline diameter of 100 m is shown (Equation 1) as well as limits to this force for average stamukha freeboard in excess of that required for hydrostatic balance (i.e. $H - d\,\rho_w / \rho_i$ based on Equation 2). What differentiates stamukhi from other grounded features is that they tend to survive multiple ice movement events and can often last until they melt in place during spring break-up. As shown in Figure 1, an excess sail freeboard of less than 1 m on average would be sufficient to stabilize a grounded ice feature for surrounding ice thicknesses up to 0.5 m.

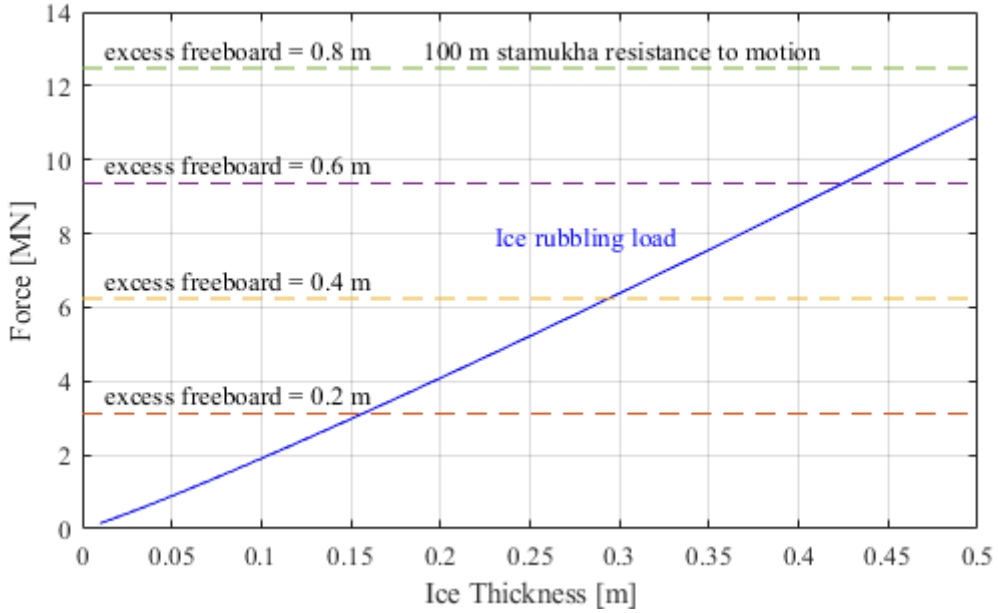

Figure 1 Resistance forces at an island or stamukha with 100 m waterline diameter based on the rubbling mechanism (Equation 1) and stability limits for stamukha sliding on the seafloor (Equation 2).

RESISTANCE TO ICE MOVEMENT AT SHORE

Depending on wind direction, the ice cover can encroach on or pull away from the shore. When the wind drives the ice away from shore, a shore crack or one somewhere in the vicinity often allows the ice to move off with little in the way of restraint. Shore cracks are a common feature for any ice environment where water level changes take place, whether due to wind surge, tides, changes in water budget in lakes or inland seas and discharge in rivers. Depending on circumstances, ice that is pushed toward shore can raft/ridge/rubble at shore or offshore, it can ride up the beach or can build rubble when the resistance to sliding exceeds the rubble-building forces.

In the finite element model, we use a gap element to allow minimal force transmission when driving forces act to pull the ice away from shore, as outlined in a subsequent section of this paper. The situation for onshore motion can be more complicated. Evidence of the mechanisms resisting onshore motion can be quite subtle. Although there is evidence of rubble build-up, significant onshore ice displacement would have been required to produce it. More importantly, one needs to identify the mechanisms that limit the stresses in the ice cover and allow the initiation of motion.

Perhaps the simplest mechanism is that the ice can slide up the beach or rocky slope. For this to take place, the ice cannot be anchored firmly to the shore, shore cracks can only have a minimal effect and buoyancy of the ice plays a role. As a result, many circumstances are likely to exist where other mechanisms are limiting. Typically, these mechanisms involve out-of-plane displacements of the ice cover. While the ice can shear or buckle in the vertical plane, these mechanisms are associated with greater forces and are more likely to take place locally than over long distances parallel to the shoreline. It is more appropriate to consider mechanisms in which the ice is lifted or pushed downward enough for the ice to ride over itself and take advantage of the minimal ice-ice friction once horizontal displacement has been initiated. For ice to be displaced onshore over significant loaded widths, it needs to be lifted or pushed down sufficiently to ride over itself. The three mechanisms – rafting, lifting and sliding – are shown in Figure 2.

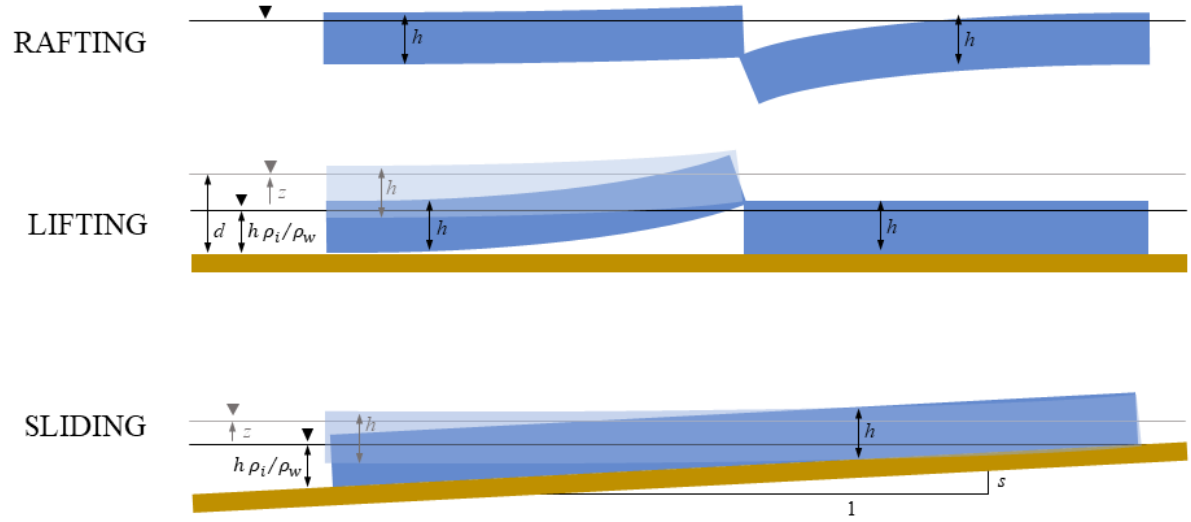

Figure 2 Potential mechanisms resisting onshore ice displacement – rafting, lifting and sliding – in which h is the ice thickness, d is the water depth, z is the increase in water level, ρ_i and ρ_w are the ice and water densities, and s is the seabed slope at the beach. The lighter shaded ice is when the change in water level, z, is greater than 0.

SLIDING AT SHORE

When the ice is pushed toward shore, the ice can potentially ride up the beach, in which case it is resisted due to the downward pressure of the ice on the gently sloping surface. In this case, the resistance depends on the distance the ice is in contact with the sea floor and the relationship between the horizontal resistance and the vertical pressure. For very cold air temperatures, the beach soil can freeze and bond (fully or partially) with the overlying ice cover.

Changes in water level can also influence the resistance to onshore ice motion. An increase in water surface elevation would decrease the ice contact distance with the sea floor, while a

decrease in the surface elevation would have the opposite effect. An increase equal to the submerged part of the ice thickness would be sufficient to reduce the resistance to zero. Even with the absence of tides, the water level in the north Caspian is seldom constant for weeks at a time and the notion of water level changes relative to a winter average can only be considered approximate. If the stiffness of the ice cover is ignored (a reasonable assumption for thin ice and shallow seabed slopes), the vertical force per unit width exerted by the ice on the seabed is

$$F_S = (g/s)[(h^2\rho_i{}^2)/(2\rho_w) - \rho_i hz + \rho_w z^2/2] \quad \text{for} \quad z \geq 0 \tag{3}$$

where g is the acceleration due to gravity, s is the seabed slope (vertical/horizontal), ρ_i is the ice density, ρ_w is the water density, h is the ice thickness and z is the water surface elevation relative to a relatively stable mean value. The second and third terms in Equation (3) account for the decrease in load as the ice is submerged and the total force is zero when the increase in water level, z, exceeds $h\,\rho_i / \rho_w$. In Equation (3), the ice is assumed to have a constant thickness, h, even when in contact with the seabed.

The forces shown in Figure 3 are calculated from Equation (3) for seabed slopes of 1/1000 and 1/100, and for ice thickness ranging up to 0.5 m. Changes in water level from zero up to $h\,\rho_i / \rho_w$, the point at which the ice is no longer in contact with the seabed, are shown in the Figure 3. Forces on the shallower slope are significantly greater because the ice is in contact with the seabed for a distance 10 times greater. Forces also increase with increasing ice thickness and decrease to zero when the ice is no longer in contact with the seabed. For comparison with the rafting and lifting mechanisms shown below, an ice-soil friction coefficient of 0.3 can be used to estimate horizontal sliding forces for a frictional soil.

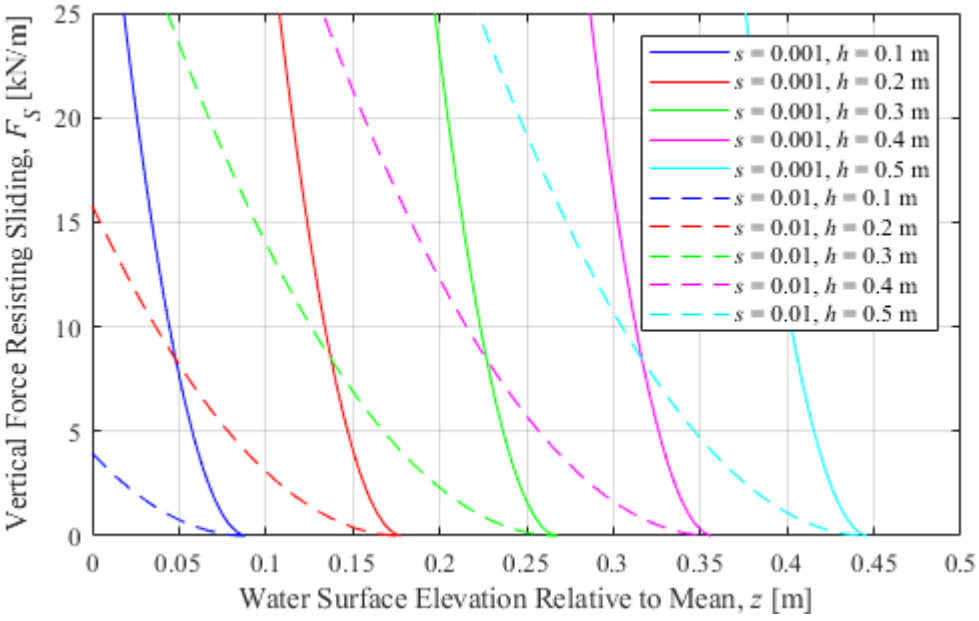

Figure 3 Vertical forces associated with sliding the ice cover in contact with the sea floor

RAFTING AND LIFTING PROCESSES

For a shallow-sloping seabed, sliding forces associated with onshore motion are quite significant (Figure 3) and it is worth considering other mechanisms that might take place. Since the sliding friction coefficient for ice on ice (typically about 0.1, ISO 19906, 2019) is less than

that on the seabed (likely to be on the order of 0.3), it is worth addressing likely mechanisms that involve ice sliding on top of ice. Two mechanisms are addressed in this section – rafting in which two floating ice sheets are pushed together and lifting in which an encroaching ice sheet is lifted over one that is stationary or frozen to the soil (see Figure 2).

The rafting and lifting problems are solved using the Euler-Bernoulli model. Because of uncertainties in all the parameters, this simple approach is used to solve the beam bending problem subjected to self-weight and buoyancy forces and various boundary conditions involving vertical displacements and derivatives thereof. In implementing this model, in-plane forces are ignored. The key parameters are the ice thickness, the elastic modulus and the moment of inertia of the cross-section. An effective elastic modulus of 2.3×10^9 N m^{-2} has been used for these calculations, to reflect relatively warm ice temperatures and slow load application.

Rafting is commonly seen in thin mobile ice and this is certainly the case in the north Caspian Sea. When an ice cover is subjected to compressive forces, one side of a pre-existing or new crack will be pushed downward while the other will be lifted so that the two sides slide on top of each other. The critical point in this mechanism is when the top surface of the side that is pushed downwards just slides under the lifted side, as shown in Figure 2. At this point, the vertical deflection of the lifted side minus the vertical deflection of the depressed side equals the thickness of the ice, and the upward and downward forces are equal. The process is illustrated in Figure 4. The vertical forces associated with the rafting process, represented by the large dots, are at the intersection of the dashed lines involving the force to push the ice downwards and the solid lines associated with upward of lifting forces. Because the ice floods under a small downward force, the ice is pushed down 0.77 times the ice thickness and lifted 0.23 times the thickness at the point of intersection. While ice thicknesses up to 0.5 m are shown in the calculations for Figure 4, mechanisms other than rafting are often seen in the upper part of this range.

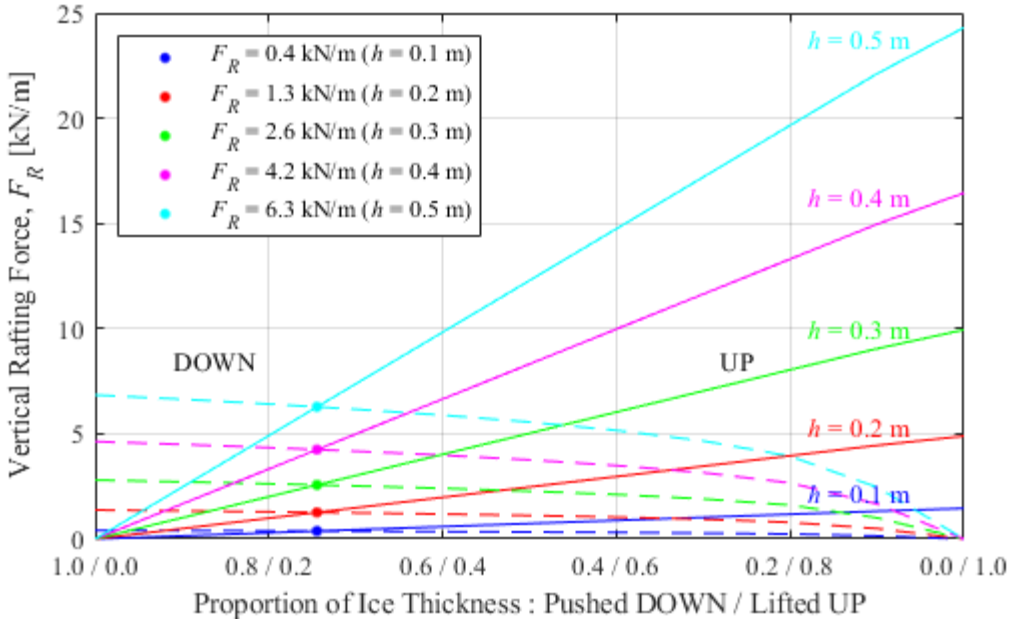

Figure 4 Vertical rafting forces for a range of ice thicknesses

A lifting mechanism is shown in Figure 2, whereby moving ice is pushed toward ice of the same thickness anchored to a shallow sloping seabed or shore and just lifted over top of it. The lifting forces for different ice thicknesses and for different water depths are given in Figure 5. The point where the lines intersect the vertical axis is when the moving ice has no buoyant force. As the water level rises, the buoyancy has an increasing effect resulting in the curved portions of the lines. Once the moving ice is floating, i.e. $d > h\,\rho_i / \rho_w$, there is a linear decrease in the vertical force with water depth until the moving ice can drift over top of the ice anchored to the seabed, in which case there is no vertical force.

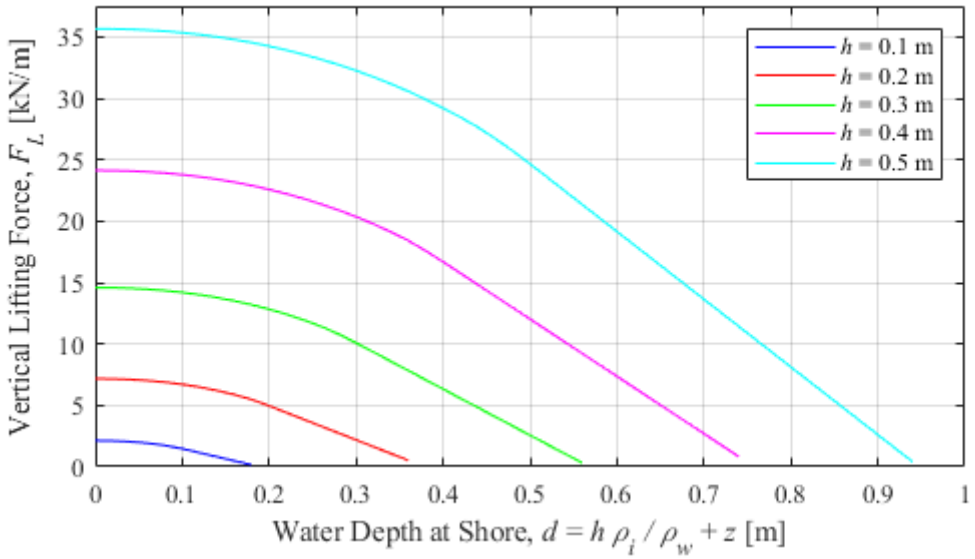

Figure 5 Lifting forces associated with ice of different thicknesses for a range of water depths

An average value for the ice-ice sliding friction coefficient is 0.1 (e.g. ISO 19906, 2019). As a result, the horizontal forces associated with rafting and lifting can be calculated from the vertical forces multiplied by the factor 0.1. Rafting and lifting forces are far less than sliding forces (Figure 3, multiplied by a friction coefficient of 0.3) and the only circumstances where the sliding forces will govern is when the ice is not anchored to the seabed nor impeded by anchored ice, and when the water level rise is sufficient to reduce the length in contact with the slope to minimize sliding forces. Because of this, sliding forces are ignored and the resistance force associated with ice movement toward shore used in the finite element calculations is the ice-ice friction coefficient of 0.1 times the lesser of the vertical forces given in Figures 4 and 5. When doing so, it is acknowledged that rafting might not occur over the entire loaded width and the maximum lifting force (zero water depth) is assumed over 10 percent of the loaded width. When interpreting Figure 5, the water level, z, associated with the lifting mechanism shown in Figure 2 is interpreted as the change from the winter mean level.

FINITE ELEMENT MODELLING

The finite element modelling approach is described in McKenna et al (2021) and in McKenna and Crocker (2021). In the present paper, the ice cover is modelled as an isotropic elastic material in plane stress. Preliminary checks indicated that delayed elastic and viscous contributions to ice deformation had a negligible effect on the results. Constant strain triangles are used for the continuum elements to allow for a random orientation of the edges. The primary function of the continuum elements is to characterize load sharing between island, stamukha and shore nodes.

On a scale of tens of kilometres, the presence of random cracks can often prevent the transmission of tensile stresses in an ice cover. This is particularly relevant for a thin ice cover subjected to water level changes, such as in the north Caspian Sea. Since stamukhi, other ice rubble features, islands and shorelines are represented by initially fixed nodes in the finite element mesh, a "gap" node is placed at each junction of the continuum elements. Gap elements (see McKenna et al, 2021) are used to link the gap nodes to the adjacent nodes of the continuum elements. This is shown schematically in Figure 6 for 3-node triangular continuum elements. Each face of a continuum element is bounded by a gap element, and the gap node at the junction of continuum elements is common to each of the surrounding gap elements. Each gap is initially closed and able to transmit forces, and then allowed to separate over the course of the simulation.

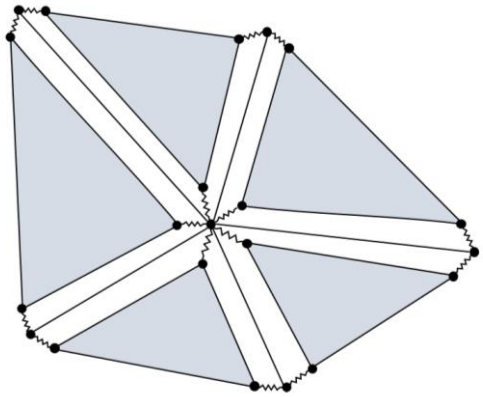

Figure 6 Four-node gap elements linking nodes of adjacent triangular elements and gap nodes where displacement boundary conditions can be applied. Although only axial springs are shown, each pair of nodes of the gap elements is linked by springs acting tangentially and perpendicularly to the sides of the adjacent triangular elements.

The wind force vector at continuum element centroids is calculated using the relationship

$$\boldsymbol{F}_a = \rho_a \, C_a \, A \, |\boldsymbol{U}| \, \boldsymbol{U} \tag{4}$$

where $\boldsymbol{U}$ is the surface wind vector, A is the surface area of the element, C_a is the drag coefficient (assumed to be 0.001 for a relatively smooth ice surface) and ρ_a is the air density. Currents are negligible in the north Caspian Sea as is water drag at the point in time when ice motion is initiated.

Displacement boundary conditions are applied only to nodes linking the gap elements (e.g. the central node attached to five others in Figure 6), not at the vertices of the continuum triangular elements. Boundaries can involve island nodes (Equation 1), stamukha nodes (Equations 1 and 2), or shore nodes (a combination of rafting and lifting forces (from Figures 4 and 5, as described above). For the shore nodes, the reaction forces are calculated per unit width and then multiplied by summing half the lengths of the adjacent gap elements to obtain a force. Typically, reaction forces at shore nodes are only relevant for onshore motion. For offshore motion, reaction forces at shore tend to be negligible because the adjacent gap elements can open. At the start of a simulation, a zero-displacement boundary condition is applied at island, stamukha or shore nodes. When the reaction force reaches the relevant limiting value, the boundary node is then allowed to displace an amount to accommodate the reduced reaction

force. Limits on the boundary reaction forces provide an energy sink to the system such that the sum of the reaction forces is less than the sum of the applied wind forces.

EXAMPLE SITUATIONS

The model described above has been tested under a range of wind, water level, bathymetric, stamukha and island situations. An approximately square region, 10 km x 10 km in extent, is used as the basis for the results shown in this paper. The ice cover is discretized as an assembly of randomly generated triangular finite elements, all joined with the gap elements described above. The continuum and gap elements are all assigned a constant ice thickness of 0.25 m. The stiffness at each end of a gap element is assigned a value of 2×10^8 N/m^3, which is then multiplied by the ice thickness and by half the length of the element to give a stiffness in N/m. In each of the situations described below, the mean water depth is 3 m over the entire area, the deviation in water level is increased linearly from zero to +0.5 m over 24 h (regardless of wind direction) and the wind speed is increased from 0 to 30 m/s linearly over 24 h as well.

The first modelled situation involves westerly winds and shore nodes on the eastern boundary, and where the nodes on the other boundaries can displace freely without reaction forces. For a 24 h simulation, all of the shore nodes reach limiting force values in less than 5 h when the wind has risen to about 6 m/s. With the rise in water level, the reaction forces at the shore nodes start decreasing when the water level rise is about 0.2 m and are zero when the water level rises to the full ice thickness of 0.25 m at 12 h.

The second modelled situation involves easterly winds and shore nodes on the northern, eastern and southern boundaries. As well, two islands (200 m waterline diameter) and one stamukha (100 m waterline diameter, total thickness 3.75 m, porosity 0.25) are placed near the centre of the region. The first cracks or open gaps appear at about 6 h, corresponding to a 7.5 m/s wind speed and a water level rise of 0.125 m. The stamukha starts to slide when the water level rise reaches 0.21 m and provides no further resistance when the water level rise is 0.35 m (Equations 1 and 2). The reaction forces at the islands cease to increase at a time of 18 h (Equation 1), corresponding to a wind speed of 22.5 m/s. In addition to the islands and stamukha, reaction forces are also activated at some of the shore nodes on the northern and southern boundaries. The finite element layout is illustrated in Figure 7, in which the crack patterns are shown at a simulation time of 18 h. The first cracks formed adjacent to the islands and subsequent ones formed adjacent to the eastern shore and downwind of the islands. Cracks are suppressed upwind of the islands where the ice cover is compressed.

CONCLUSIONS AND DISCUSSION

Using a continuum elastic model of the ice cover as a basis, a representation of ice behaviour at a 1 km resolution has been achieved through the introduction of gap elements at all boundaries between continuum finite elements to represent pre-existing cracks. In addition, gap nodes have been introduced to represent islands, stamukhi and other grounded rubble features, as well as constraints at shore. A particular feature of the approach is the calculation of finite boundary displacements to balance force thresholds due to limits imposed by rafting and lifting of the ice adjacent to shore, floating of grounded rubble features with water level rise, and ice rubbling processes at islands and stamukhi.

The example situations shown in the paper are intended solely to illustrate the approach. More realistic situations using actual data for the north Caspian Sea are modelled in McKenna et al (2023). In the present model, the ice cover can pull apart (i.e. form leads) when gap elements

open up, thereby limiting the tensile strength to very small values averaged over a number of elements. Significant deformations can therefore only occur at the boundary nodes, representing ice processes involving rubbling, sliding on the sea floor, rafting and lifting. No attempt has been made to represent other deformation and failure processes within the ice cover.

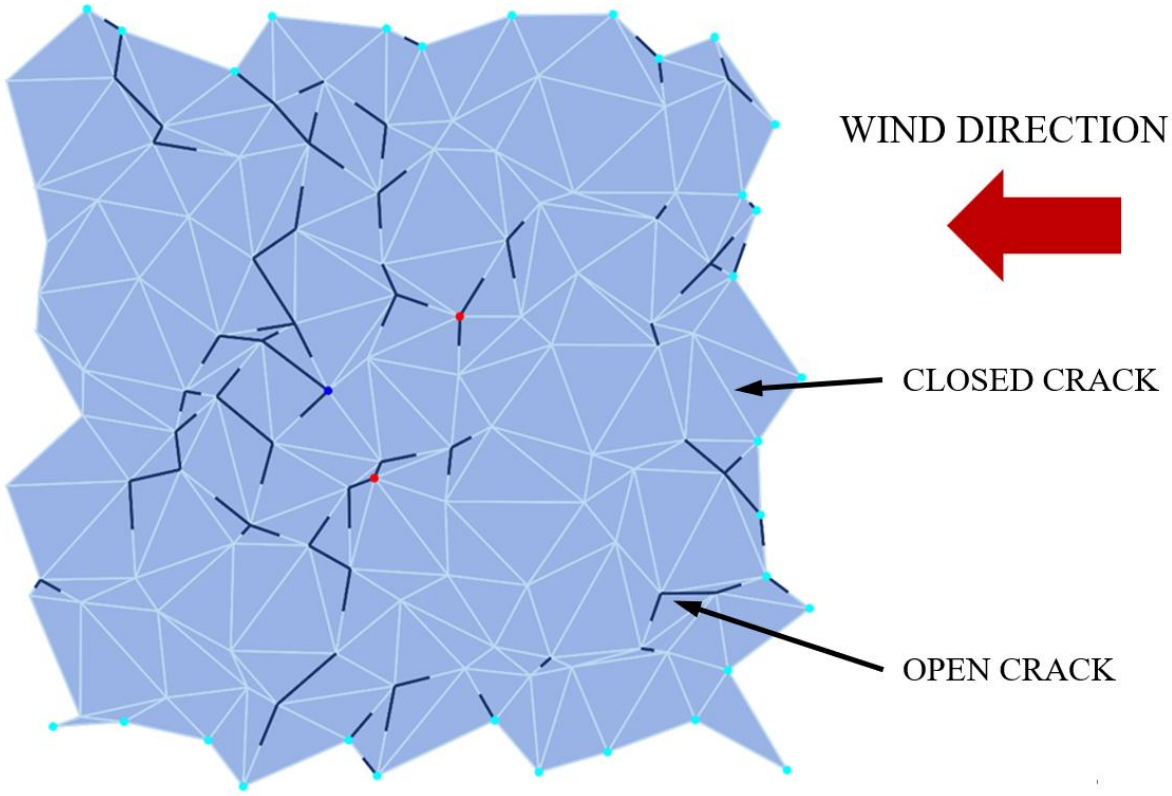

Figure 7 Example of crack patterns in a 10 km x 10 km region at 18 h, water level rise 0.375 m, wind speed 22.5 m/s (shore nodes ●, island nodes ●, stamukha node ●)

The example situations shown in the paper are intended solely to illustrate the approach. More realistic situations using actual data for the north Caspian Sea are modelled in McKenna et al (2023). In the present model, the ice cover can pull apart (i.e. form leads) when gap elements open up, thereby limiting the tensile strength to very small values averaged over a number of elements. Significant deformations can therefore only occur at the boundary nodes, representing ice processes involving rubbling, sliding on the sea floor, rafting and lifting. No attempt has been made to represent other deformation and failure processes within the ice cover.

One of the main objectives of the modelling technique is to estimate wind speed/direction and water level change thresholds that can principate the initiation of motion for a stationary ice cover. It is emphasized that the model is not intended to predict subsequent drift speeds. Because deformation processes within the ice cover are not modelled, calculated ice displacements are not realistic either. The continuum elastic ice behaviour is merely a computational convenience and ice displacements are underestimated. Much better models exist for representing ice cover displacements and drift. Nevertheless, the approach provides a reasonable way of representing the balance of forces for complex shoreline geometries, multiple islands and stamukhi, realistic bathymetries, as well as temporally varying winds and water level changes. With the present approach, it might be convenient in future to represent compressive and shear failure (i.e. ridging) within the ice cover by adapting the gap element behaviour.

How does the present model represent the initiation of ice motion? First of all, any shore, island and stamukha nodes reaching the limiting forces described in the paper can be associated with some local ice motion. For some decision-making purposes, activation of the limiting forces at multiple boundary locations might be required. Another indication of ice motion is the disintegration of the ice cover evidenced by open cracks, as in the area downwind of the stamukha in the Figure 7 example and at other specific locations near the shore and the islands (see McKenna et al, 2023).

REFERENCES

Croasdale, K.R., 2012. Ice rubbling and ice interaction with offshore facilities, *Cold Regions Science and Technology*, Vol. 76-77, pp.37-43, http://dx.doi.org/10.1016/j.coldregions.2011.06.005

ISO 19906, 2019. *Petroleum and natural gas industries — Arctic offshore structures*, International Organization for Standardization.

McKenna, R., Crocker, G. and Loewen, A., 2021. A finite element model for the deformation of floating ice covers, *Cold Regions Science and Technology*, Vol. 182, https://doi.org/10.1016/j.coldregions.2020.103213

McKenna, R. and Crocker, G., 2021. Effective moduli for flexure of a floating ice cover due to temperature variations through the depth of the ice, in *Proceedings of the 26th International Conference on Port and Ocean Engineering under Arctic Conditions*, Moscow, Russia.

McKenna, R. Kadranov, E., Sigitov, A. and Vernyayev, S. 2023. Forces associated with the initiation of ice movement events in the north Caspian Sea, in *Proceedings of the 27th International Conference on Port and Ocean Engineering under Arctic Conditions*, Glasgow, U.K.

Palmer, A.C. and Croasdale, K.R., 2013. *Arctic offshore engineering*, World Scientific Publishing Co Pte Ltd, 357 p.